Atticle ID：1003-501X(2009)07-0050-05

Characteristics of Spectral Radiance Measured by Imaging Spectrometer with Motion Compensation

FENG Yu-tao[1, 2]，XIANG Yang[1]，CHEN Xu[1, 2]

(1. *State Key Laboratory of Applied Optics*, *Changchun Institute of Optics*, *Fine Mechanics and Physics*, *CAS*, *Changchun* 130033, *China*; 2. *Graduate School of Chinese Academy of Sciences*, *Beijing* 100039, *China*)

Abstract: In order to study the characteristics of spectral radiance measured by imaging spectrometer with motion compensation, the relationship between measured radiance and the tilt angle of the axis of Instantaneous Field of View (IFOV) was derived. In the Visible-near Infrared (VNIR) (0.4~1.0 μm), the ratio of the spectral radiance measured by imaging spectrometer with a certain tilt angle α to that with tilt angle α=0º (corresponding to observing nadir point) was calculated. Compared with observing nadir point (tilt angle α=0º), the measured total radiance decreases with the tilt angle α increasing in the process of motion compensation. And the proportion of measured target radiance in measured total radiance also becomes small. In order to make the increment of measured radiance keep or approach the gain by design in the process of motion compensation, the tilt angle of axis of α should be less than 30º.

Key words: imaging spectrometer; remote sensing imaging; optical axis swing angle; motion compensation

CLC number: TP702; TH744 **Document code**: A doi：10.3969/j.issn.1003-501X.2009.07.010

运动补偿下成像光谱仪的辐射能量采集特性

冯玉涛[1,2]，向 阳[1]，陈 旭[1,2]

(1. 中国科学院长春光学精密机械与物理研究所, 应用光学国家重点实验室, 长春 130033;
2. 中国科学院研究生院，北京 100039)

摘要: 为研究运动补偿下成像光谱仪的辐射能量采集特性，首先推导出系统探测器像元采集到的光谱辐射能量与瞬时视场光轴摆角的关系式。据此，在可见近红外(0.4～1.0 μm)光谱范围内，计算不同摆角下系统采集到的光谱辐射能量与观测星下点(对应光轴摆角为 0º)时系统采集到的光谱辐射能量的比值。结果表明：与观测星下点相比，运动补偿过程中系统采集到的总光谱辐射能量随光轴摆角的增大而减小，并且其中地面目标辐射所占的比例也随之减小。系统信噪比有类似的特性。要使整个观测过程辐射能量提高的倍率保持或接近预期的补偿倍率，光轴摆角尽量小于 30º。

关键词: 成像光谱仪；遥感成像；光轴摆角；运动补偿

0 Introduction

An Imaging spectrometer measures the image of ground scene pixels and simultaneously obtains spectral data of each scene pixel in tens to hundreds contiguous spectral bands [1-2]. The spectral radiance measured by detector pixels of an imaging spectrometer would be little for observing water or low albedo target. It is anticipated to prolong the integral time of detector to increase the Signal-to-Noise Ratio (*SNR*) of the imaging spectrometer. Motion Compensation (MC) method is generally used to increase integral time of detector such as

收稿日期：2008-12-17; **收到修改稿日期**：2009-02-26

基金项目：国家自然科学基金重点项目(60538020)

作者简介：冯玉涛(1980-)，男(汉族)，吉林长春人。博士研究生，主要从事超光谱成像系统性能分析和设计等方面的研究。
E-mail: fytciom@126.com。

COIS [3], Hyperion [4] and HIRIS [5]. The principle of MC is shown in fig.1. When the pointing mirror is laid 45°, imaging spectrometer observes nadir point. When the space-borne imaging spectrometer lies in position 1, the pointing mirror turns $\alpha/2$ ahead. So the axis of Instantaneous Field Of View (IFOV) is turned ahead α along flight direction and points to D_1 before the nadir point B_1. And then the axis of IFOV is turned backwards relative to the imaging spectrometer by controlling pointing mirror. Until position 3, motion compensation is completed. The point mirror is quickly turned ahead again and the axis of IFOV points to B_2. Next motion compensation is beginning. If the distance from position 1 to 3 is $A_1B_1=nl$ and the observed distance is $C_1D_1=l$, the integral time of detector will increase n times compared with without MC for observing scene area C_1D_1. Using MC can increase SNR of an imaging spectrometer. But it makes spatial resolution some loss [5]. In addition, the geometrical ubiety of ground scene pixel relative to the entrance pupil of imaging spectrometer and the transmission path of scene radiance would change with the Tilt Angle of the Axis of IFOV (hereafter, TAA for short). Further, the measured scene radiance and atmosphere scatter radiance are varied with TAA. The characteristics of spectral radiance measured by imaging spectrometer with MC will be analyzed concretely in the following sections.

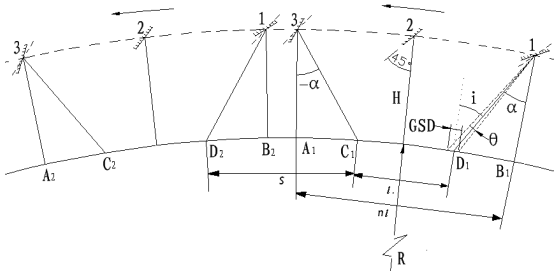

Fig.1　Sketch map of motion compensation

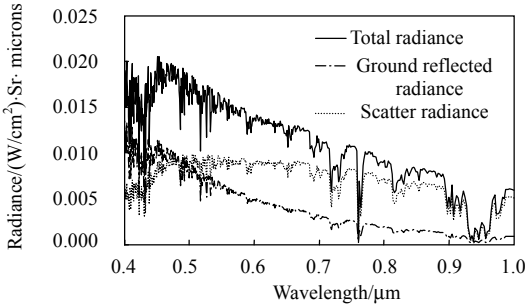

Fig.2　Upwelling spectral radiance from nadir point to the entrance pupil

1　Theoretical Discussion

For a spaceborne push-broom imaging spectrometer without MC, the measured radiance Φ of the detector pixel is the convolution of the spectral response function $f(\lambda-\lambda_0)$ with a high-resolution upwelling spectrum $L(\lambda)$ across the spectral band:

$$\Phi = T_{\text{int}}\tau_{\text{opt}}\int L(\lambda)f(\lambda-\lambda_0)\mathrm{d}\lambda\cdot\cos i\cdot\Delta S\cdot\Delta\omega \tag{1}$$

Where, T_{int} is integral time of detector. $L(\lambda)$ is upwelling spectral radiance. The spectral response function generally is Gaussion function. τ_{opt} is transmittance of optical system. cos$i$ is cosine of the included angle between ground pixel normal and the axis of IFOV. For imaging spectrometer without MC, i=0°, cos$i$=1. $\Delta S=GSD_{\text{nadir}}^2$ is ground pixel area. GSD_{nadir} is Ground Sampling Distance (spatial resolution) corresponding to nadir point. $\Delta\omega=\pi D^2/4H^2$ is the solid angle of entrance pupil to ground pixel. D is diameter of entrance pupil of imaging spectrometer system. H is the height of space orbit.

The definition of the angle of IFOV θ is given by

$$\tan\frac{\theta}{2}=\frac{d}{2f}=\frac{GSD_{\text{nadir}}}{2H} \tag{2}$$

When the dimension of detector pixel d, focal length of telescopic system f and the height of space orbit H are fixed, the IFOV and GSD_{nadir} also become fixed value. So cos$i$, ΔS and $\Delta\omega$ are invariable for the imaging spectrometer without MC.

For imaging spectrometer with MC, there is just one position where the system observes nadir point, while there is an included angle α (TAA) between the axis of IFOV and nadir direction in other positions. The radiance

transmission direction and path are variable. ΔS, $\Delta\omega$ and cos$i$ are variable. The relationship of ΔS, $\Delta\omega$ and cos$i$ with α can be expressed as

$$\Delta S = GSD_x \cdot GSD_y = R\{\arcsin[M\sin(\alpha+\theta/2)] - \arcsin[M\sin(\alpha-\frac{\theta}{2})]-\theta\}\cdot\frac{2H}{\cos\alpha}\tan\frac{\theta}{2} \tag{3}$$

$$\Delta\omega = \frac{(\pi D^2/4)\sin^2\alpha}{\{\sin[\arcsin(M\sin\alpha)-\alpha]R\}^2},\quad \cos i = \cos[\arcsin(M\sin\alpha)] \tag{4}$$

Where: R is the radius of the earth; M=(R+H)/R; GSD_x and GSD_y are along-track and cross-track spatial resolution. We assume that the observed ground scene surfaces are spherical surface at along-track direction and plane surface at cross-track direction.

The incident spectral radiance of imaging spectrometer with MC is given by

$$L(\lambda,\alpha) = L_g(\lambda)\tau_0(\lambda)^{m(\alpha)} + L_s(\lambda,\alpha) \tag{5}$$

Where: L_g is ground scene spectral radiance. L_s is atmosphere scatter radiance. $\tau_0(\lambda)$ is the vertical transmittance of atmosphere corresponding to nadir point. $m(\alpha)$ is the relative atmosphere mass, it can be expressed as [6]

$$m(\alpha) = \frac{1}{\cos\alpha + 0.150\,0(93.885-\alpha)^{-1.253}} \tag{6}$$

Finally, substitute Eq.(3)~(6) into Eq.(1), the relationship between the measured radiance Φ_n and TAA α for the imaging spectrometer with MC is given by

$$\Phi_n(\alpha) = \frac{\pi D^2\tau_{opt}nT_{int}H}{2R}\int[L_g(\lambda)\tau_0(\lambda)^{m(\alpha)} + L_s(\lambda)]f(\lambda-\lambda_0)\mathrm{d}\lambda\cdot\cos[\arcsin(M\sin\alpha)]\cdot \{\arcsin[M\sin(\alpha+\frac{\theta}{2})] - \arcsin[M\sin(\alpha-\frac{\theta}{2})]-\theta\}\frac{\tan(\theta/2)}{\cos\alpha}\cdot\frac{\sin^2\alpha}{\sin^2[\arcsin(M\sin\alpha)-\alpha]} \tag{7}$$

Where, n is MC gain. When α=0° and n=1, there is no MC and the system observes nadir point. Eq.(7) is the same as Eq.(1).

According Eq.(7), the equation to compute the signal in electrons per pixel is

$$N_n(\alpha) = \frac{\pi D^2 nT_{int}H\tau_{opt}\eta}{2hcR}\int[L_g(\lambda)\tau_0(\lambda)^{m(\alpha)} + L_p(\lambda)]f(\lambda-\lambda_j)\lambda\mathrm{d}\lambda\cdot\cos[\arcsin(M\sin\alpha)]\cdot \{\arcsin[M\sin(\alpha+\frac{\theta}{2})] - \arcsin[M\sin(\alpha-\frac{\theta}{2})]-\theta\}\frac{\tan(\theta/2)}{\cos\alpha}\cdot\frac{\sin^2\alpha}{\sin^2[\arcsin(M\sin\alpha)-\alpha]} \tag{8}$$

Where: h is Planck constant. c is light speed. η is quantum efficiency of detector. The SNR of the imaging spectrometer with MC also varies with the tilt angle of the axis of IFOV α. The expression of SNR is

$$SNR = N_n/\sqrt{N_{oe}^2 + N_e^2} \tag{9}$$

Where N_{oe}=$N_n^{1/2}$ is the photon-to-electron conversion noise [7]. N_e is the electronic noise.

2 Calculations and Discussions

In order to analyze the characteristics of spectral radiance measured by imaging spectrometer with MC, the upwelling ground scene spectral radiance, scatter radiance and the total spectral radiance at the top of the atmosphere were modeled in the spectral range of 0.4~1.0 μm with conditions of a 30° solar illumination angle, a 0.3 reflection horizontal surface at sea level, and the 23 km visibility, standard mid-latitude summer atmosphere model (See Fig.2) [8]. The spectral resolution is 10 nm. The height of orbit is H=400 km. The radius of the earth is R=6 378.01 km. The gain of MC is n=2. The ratios of measured radiance $\Phi_2(\alpha)$/ $\Phi_2(0°)$ between a certain TAA α and observing nadir point (α=0°) are calculated according Eq.(7) (see Fig. 3 to 5).

Fig.3 shows the ratio of measured scene radiance with a certain TAA α to that with observing nadir point

(α=0°). The measured scene radiance decreases along with α increasing in the process of motion compensation. When α increases, the transmission path of scene radiance in the atmosphere becomes longer. The absorption and scatter of atmosphere become stronger. There is more energy loss for scene radiance in transmission. The signal level of target radiance measured by imaging spectrometer also becomes lower. When α is less than 30°, the average reduction of measured scene radiance is no more than 10%. When α=45°, the average reduction of measured scene radiance is near 20% and more than 20% in short-wave spectral range.

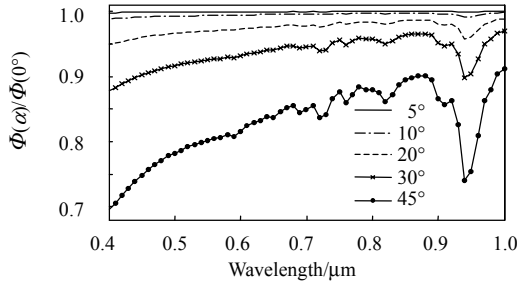

Fig.3　The gain of MC is n=2，the ratio of measured ground scene radiance $\Phi_2(\alpha)/\Phi_2(0^\circ)$

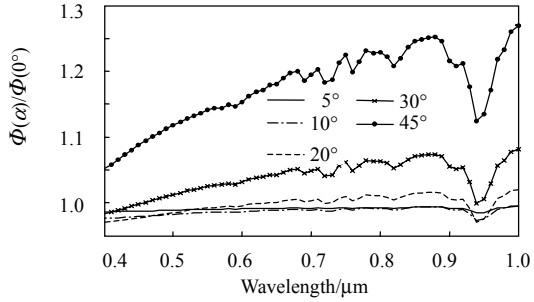

Fig.4　The gain of MC is n=2，the ratio of measured atmosphere scatter radiance $\Phi_2(\alpha)/\Phi_2(0^\circ)$

Fig.4 shows the ratio of measured scatter radiance with a certain TAA α to that with observing nadir point (α=0°). The measured scatter radiance firstly decreases and afterward increases along with α increasing. This characteristic is determined by the geometrical relationship of observer-target-sun. When α is less than 30° the average variation of measured scatter radiance is no more than 5%. When α=45°, the average increment of measured scatter radiance is 15%. The disturbance of the scatter radiance to the scene radiance is strengthened obviously.

Fig.5 shows the ratio of measured total radiance with a certain TAA α to that with observing nadir point (α=0°). The measured total radiance always decreases along with α increasing in the process of motion compensation. It indicates that the reduction of measured scene radiance is lager than the increment of measured scatter radiance. Although the average reduction of measured total radiance is no more than 8% when α<45°, the proportion of ground scene radiance in total radiance becomes smaller compared with observing nadir point (α=0°). The capability to detect the ground scene cannot maintain two times MC gains by design along with α increasing. So the maximum of α is better no more than 30° when using MC. Fig.6 shows increase ratio of *SNR* of imaging spectrometer between with and without MC corresponding to different MC gain and α. The parameters of imaging spectrometer used to calculate *SNR* are listed in Table 1[5]. When using MC, the increase values of *SNR* corresponding to observing nadir point (α=0°) are approximately proportional with the square root of MC gain n. For a certain MC gain, *SNR* decreases along with α increasing. When α=45° *SNR* averagely decrease 15% (Fig.6).

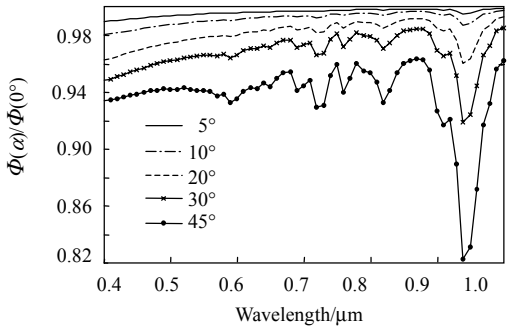

Fig.5　The gain of MC is n=2，the ratio of measured total radiance$\Phi_2(\alpha)/\Phi_2(0°)$

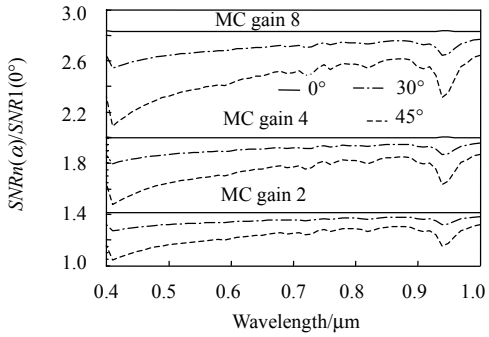

Fig.6　*SNR* increase gains corresponding to different MC gains and α

The relationship of MC gain n, observing distance l and the maximum of TAA (α_{max}) can be expressed as

$$\arcsin(M\sin\alpha_{max})-\alpha_{max}=(n-1)L/2R \tag{10}$$

Eq.(10) indicates that: For a certain α_{max}, if MC gains n increase, the observing distance l will decrease. If the observing distance l keeps invariable, increasing MC gain n must enlarge α_{max}. But When α>30°, the measured total radiance and the proportion of scene radiance are much smaller than that with observing nadir point (α=0°). The detective capability for the scene target cannot reach n times MC gain by design. Table 2 lists the observing distance in MC with certain MC gain and α_{max}.

Table 1 Systematic parameters of HIRIS

Parameters	Value
H	824 km
GSD	30 m
Integral time	4.55 ms
Aperture	376 mm
Focal ratio	F/3.8
Pixel size	52 micron
Readout noise	<300 electrons rms
Dark current	Negligible
Spectral coverage	400~1 000 nm
Average spectral resolution	9.4 nm
Quantum efficiency	>40%

Table 2 Observing distance l (unit km) corresponding to different the maximum of TAA (α_{max}) and MC gain n

α_{max}	MC gain		
	2	4	8
30°	973.87	324.62	139.12
45°	1 777.4	592.46	253.91

3 Conclusions

Using motion compensation can prolong the integral time of detector and finally increase the SNR of imaging spectrometer. While the geometrical relationship of ground target to imaging spectrometer and the transmission path of spectral radiance are changed because of the swing of the point mirror. the total radiance measured would decrease along with the tilt angle of axis of IFOV increasing in the process of motion compensation. And the proportion of ground scene radiance in total radiance also becomes smaller. Just when observing nadir point (α=0°) the increase of *SNR* can reach the value by design. In order to make the detective capability of imaging spectrometer to approach the increase value with MC, the tilt angle of the axis of IFOV is better no more than 30°.

Reference:

[1] Goetz A F H，Vane G，Solomon J E，*et al*. Imaging spectrometry for earth remote sensing [J]. **Science**(S0036-8075)，1985，**228**(4704)：1147−1153.

[2] 金锡哲，向阳，禹秉熙. 三角共路型干涉成象光谱仪研究 [J]. 光电工程，2001，**28**(2)：14−18.
JIN Xi-zhe，XIANG Yang，YU Bing-xi. Research on Triangle Common-Path Type Imaging Fourier Transform Spectrometer [J]. **Opto-Electronic Engineering**，2001，**28**(2)：14−18.

[3] Wilson T，Davis C. Naval EarthMap Observer (NEMO) Satellite [J]. **Pro. of SPIE**(S0277-786X)，1999，**3751**：2−10.

[4] Pearlman J，Segal C. Development and operations of the EO-1 hyperion imaging spectrometer [J]. **Pro. of SPIE**(S0277-786X)，2004，**4135**：243−253.

[5] Goetz A F H，Herring M. The High Resolution Imaging Spectrometer (HIRIS) for Eos [J]. **IEEE transaction on geosciences and remote sensing**(S0196-2892)，1989，**27**：136−144.

[6] Blattnew W G，Henry G Horak, Dave G Collins，*et al*. Monte Carlo Studies of the Sky Radiation at Twilight [J]. **Appl. Opt**(S0003-6935)，1974，**13**(3)：534−537.

[7] Eckardt A，Hofer S. SNR Estimation for Advanced Hyperspectral Space Instrument [J]. **SPIE**(S0277-786X)，2005，**5883**：1−7.

[8] Guanter L，Víctor Estellés，Moreno J. Spectral calibration and atmospheric correction of ultra-fine spectral and spatial resolution remote sensing data application to CASI-1500 data [J]. **Remote Sensing of Environment** (S0196-2892)，2007，**109**(1)：54−65.